

KAT2A complexes ATAC and SAGA play unique roles in cell maintenance and identity in hematopoiesis and leukemia

Liliana Arede,^{1,2} Elena Foerner,^{1,*} Selinde Wind,^{1,*} Rashmi Kulkarni,¹ Ana Filipa Domingues,¹ George Giotopoulos,^{1,3} Svenja Kleinwaechter,¹ Maximilian Mollenhauer-Starkl,⁴ Holly Davison,⁴ Aditya Chandru,² Ryan Asby,^{1,3} Ralph Samarista,⁴ Shikha Gupta,^{1,2} Dorian Forte,^{1,5} Antonio Curti,⁶ Elisabeth Scheer,⁷⁻⁹ Brian J. P. Huntly,^{1,3} Laszlo Tora,⁷⁻⁹ and Cristina Pina^{4,10}

¹Department of Haematology, ²Department of Genetics, and ³Wellcome-MRC Cambridge Stem Cell Institute, University of Cambridge, Cambridge, UK; ⁴College of Health, Medicine and Life Sciences, Division of Biosciences, Brunel University London, Uxbridge, UK; ⁵Department of Experimental, Diagnostic, and Specialty Medicine (DIMES), Institute of Hematology "Seràgnoli", Bologna, Italy; ⁶IRCCS Azienda ospedaliero-universitaria di Bologna, Istituto di Ematologia "Seràgnoli", Bologna, Italy; ⁷Institut de Génétique et de Biologie Moléculaire et Cellulaire, Illkirch, France; ⁸Centre National de la Recherche Scientifique (CNRS), UMR7104, Illkirch, France; ⁹Institut National de la Santé et de la Recherche Médicale (INSERM), U1258, Illkirch, France; and ¹⁰Centre for Genome Engineering and Maintenance (CenGEM), Brunel University London, Uxbridge, UK

Key Points

- KAT2A is required at different stages of human cord blood erythroid development with ATAC and SAGA complex specificity.
- KAT2A regulates leukemia cell maintenance and identity through specific participation in ATAC and SAGA complexes.

Epigenetic histone modifiers are key regulators of cell fate decisions in normal and malignant hematopoiesis. Their enzymatic activities are of particular significance as putative therapeutic targets in leukemia. In contrast, less is known about the contextual role in which those enzymatic activities are exercised and specifically how different macromolecular complexes configure the same enzymatic activity with distinct molecular and cellular consequences. We focus on KAT2A, a lysine acetyltransferase responsible for histone H3 lysine 9 acetylation, which we recently identified as a dependence in acute myeloid leukemia stem cells and that participates in 2 distinct macromolecular complexes: Ada two-A-containing (ATAC) and Spt-Ada-Gcn5-Acetyltransferase (SAGA). Through analysis of human cord blood hematopoietic stem cells and progenitors, and of myeloid leukemia cells, we identify unique respective contributions of the ATAC complex to regulation of biosynthetic activity in undifferentiated self-renewing cells and of the SAGA complex to stabilization or correct progression of cell type-specific programs with putative preservation of cell identity. Cell type and stage-specific dependencies on ATAC and SAGA-regulated programs explain multilevel KAT2A requirements in leukemia and in erythroid lineage specification and development. Importantly, they set a paradigm against which lineage specification and identity can be explored across developmental stem cell systems.

Introduction

KAT2A is a histone acetyltransferase required for correct mesodermal specification in the developing mouse embryo.¹ It stabilizes pluripotency of mouse embryonic stem (ES) cells² and is required for survival of neural stem and progenitor cells.³ In hematopoiesis, Kat2a has been shown to regulate proliferation and activation of T-cell subsets⁴ and maturation of invariant natural killer T (iNKT) cells,⁵ and it

Submitted 2 July 2020; accepted 20 September 2021; prepublished online on *Blood Advances* First Edition 15 October 2021; final version published online 7 January 2022. DOI 10.1182/bloodadvances.2020002842.

*E.F. and S.W. contributed equally to this study.

ChIP-seq and A-seq data have been deposited in GEO (accession numbers GSE128902 and GSE128512).

Send data sharing requests via e-mail to the corresponding author.

The full-text version of this article contains a data supplement.

© 2022 by The American Society of Hematology. Licensed under Creative Commons Attribution-NonCommercial-NoDerivatives 4.0 International (CC BY-NC-ND 4.0), permitting only noncommercial, nonderivative use with attribution. All other rights reserved.

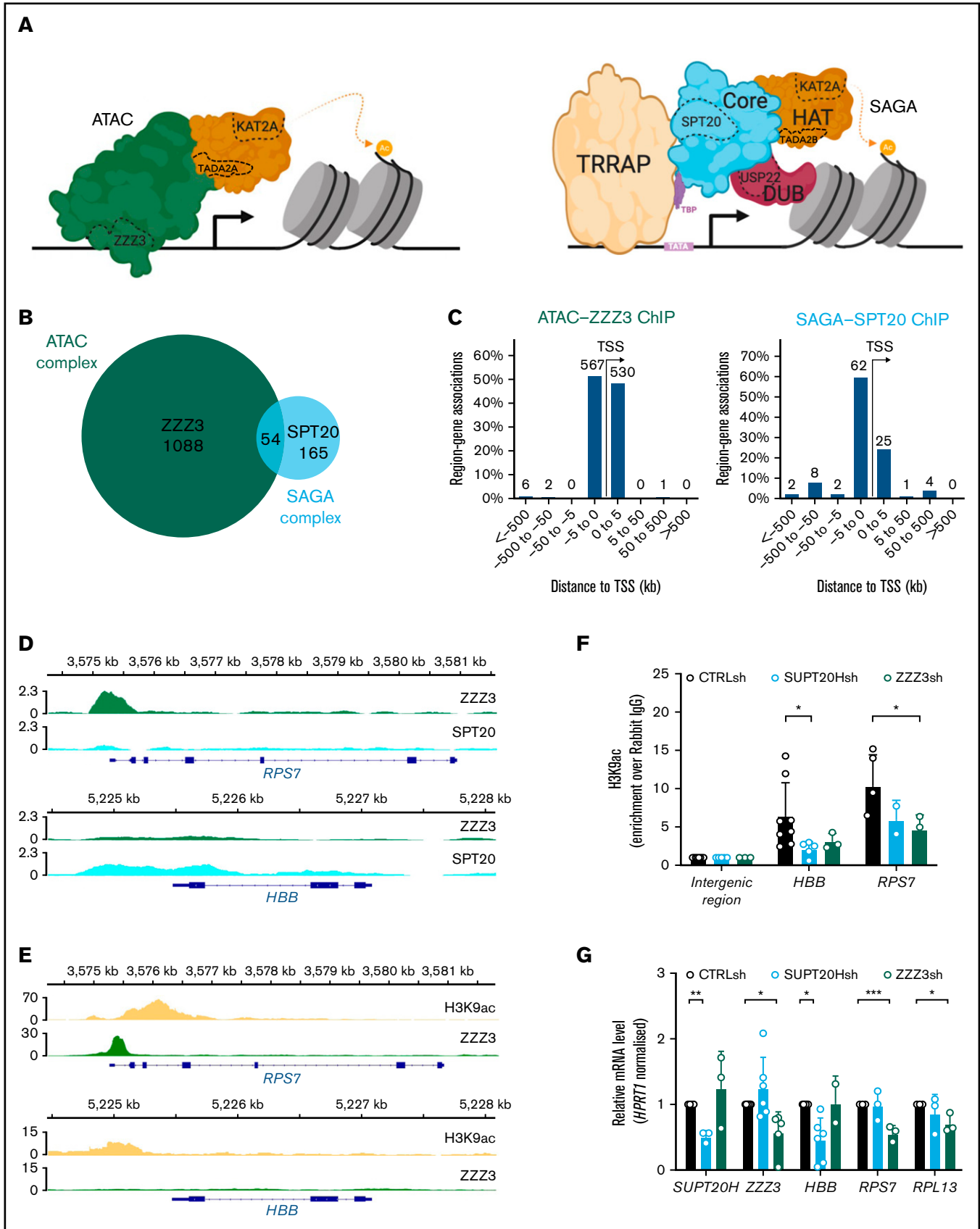


Figure 1. KAT2A-containing ATAC and SAGA complexes have unique targets in hematopoietic cells. (A) Schematic representation of the human ATAC (left) and SAGA (right) multiprotein complexes. SAGA (right) is organized into distinct structural and functional modules, colored similarly. The KAT2A-containing histone

restricts terminal differentiation of granulocytic cells.⁶ We⁷ and others⁶ have not found that *Kat2a* play a central role in hematopoietic stem cells. In contrast, we have identified KAT2A as a requirement in acute myeloid leukemia (AML) cell lines and patient samples.⁸ Using a conditional knockout mouse model, we showed that *Kat2a* loss results in transcriptional instability of general metabolic regulation programs such as translation and ribosomal protein synthesis, leading to probabilistic loss of functional leukemia stem-like cells.⁷ *Kat2a* exerts transcriptional control through histone or nonhistone lysine acetylation, including in the examples cited within the hematopoietic system. Specifically, regulation of leukemia stem-like cells⁷ and control of T-cell subset activation⁴ are linked to histone H3 lysine 9 acetylation (H3K9ac) at gene promoters, a role that is evolutionarily conserved from the original identification of *Gcn5* in yeast⁹ and associated with transcriptional activation.¹⁰ Granulocytic and iNKT cell maturation, on the other hand, depend on protein acetylation of key transcriptional regulators, respectively *Cebpa*⁶ and *Egr2*.⁵ More recently, *Kat2a* has been shown to catalyze histone succinylation, another acyl modification that, like H3K9ac, is associated with transcriptional activation.¹¹

KAT2A exerts its activity in the context of 2 macromolecular complexes, Ada-Two-A-Containing (ATAC) and Spt-Ada-Gcn5-Acetyltransferase (SAGA) (Figure 1A). These complexes share the HAT activity by KAT2A, with a single subunit difference within the HAT module (TADA2A in ATAC and TADA2B in SAGA).¹² Additionally, the 2 complexes exhibit different chromatin specificities and regulate distinct sets of genes.¹³ Integration of KAT2A in either complex is a requirement for its full HAT activity¹⁴; however, analysis of their differential contributions to KAT2A function in a given system has not been performed to date. The yeast KAT2A-containing SAGA was the first multimodular HAT complex to be isolated.¹⁰ Since then, several studies unveiled its molecular architecture: SAGA comprises 19 subunits organized in 4 functionally distinct modules¹⁵, a structure highly conserved from yeast to human.¹² In addition to the KAT2A participating HAT module, which also includes TADA2B, TADA3, and CCDC101 (SGF29), SAGA contains: (1) a H2B DUB module centered on USP22 enzymatic activity; (2) a core module comprising SPT20, which is specific to SAGA, and 5 TBP-associated factors (TAFs), 3 of which are shared with TFIID; and (3) the transcription factor interaction module, TRRAP. Two recent reports on the cryo-electron microscopy structure of the yeast SAGA complex described the interactions between the different modules with key implications for gene activation.^{16,17} The SAGA

core module contains an octamer-like fold that facilitates TBP loading onto TATA promoters¹⁷; the 2 enzymatic HAT and DUB modules connect flexibly to the core,^{16,17} suggesting functional independence between them. The ATAC complex, in turn, is exclusive to multicellular eukaryotes.¹² It was first linked to chromatin remodeling functions in *Drosophila*,¹⁸ where it preferentially targets histone H4.¹⁹ ATAC histone substrates in mammalian cells are less clear, although human ATAC preferentially modifies H3.²⁰ ATAC-specific elements include DNA-binding subunit ZZZ3, HAT module component TADA2A, and YEATS2, which is required for assembly of the ATAC complex and has acetyl-reading activity.²¹ Moreover, ATAC comprises additional HAT activity by KAT14, which is essential for ATAC assembly and required in embryonic development.²² Additionally, both KAT2A-containing complexes have been implicated in malignant transformation.²³ ATAC-YEATS2 was shown to be highly amplified in non-small cell lung cancer and required for malignant cell survival.²¹ SAGA complex cofactor TRRAP interacts with multiple proteins key to oncogenesis, such as c-Myc and E2F proteins.²⁴ Expression of SAGA *USP22* associates with an oncogenic signature of poor prognosis.²⁵ However, recent studies propose a tumor suppressor function of *USP22*,²⁶ including in AML,²⁷ suggesting dependency on cell context for functional consequences and fate decisions.

Herein, we attempted to characterize the role of KAT2A-containing ATAC and SAGA complexes in normal and leukemic blood cell function. We identified unique ATAC-specific requirements for specification or propagation of early erythroid-committed progenitors, which were distinct from the participation of the SAGA complex in progression of erythroid differentiation. In AML cells, ATAC and SAGA controlled distinct aspects of biosynthetic maintenance and identity preservation of leukemia cells, thus suggesting a dichotomy between ATAC- and SAGA-centered KAT2A functions that has implications for normal and malignant developmental decisions.

Methods

Cell lines

K562, MOLM13, and Kasumi-1 lines (kind gift from Brian Huntly, Cambridge, UK) and KG1a (kind gift from Joanna Baxter, Cambridge Blood and Stem Cell Biobank) were maintained in RPMI supplemented with 20% fetal bovine serum (FBS; Invitrogen), 1% penicillin/streptomycin/amphotericin (P/S/A; Invitrogen) and 2 mM L-Gln. HEK 293T cells were grown in Dulbecco's modified Eagle

Figure 1. (continued) acetyltransferase (HAT) module is depicted in orange and partially shared with ATAC (left), with exception of TADA2B, which is replaced by TADA2A in ATAC. The histone deubiquitination (DUB) module is shown in red; the core module, which includes SPT20, in blue. TF-binding module, TRRAP, is shown in yellow. TATA-binding protein (TBP), in purple, is not part of the complex architecture, but it associates with SUPT3H to recruit SAGA to TATA box and facilitate transcription. The ATAC complex does not have a modular organization. Its main structure is shown in green and includes DNA-binding subunit ZZZ3. Subunits tested in this study are delineated with a dashed line. (B) Venn diagram of consensus ZZZ3 and SPT20 ChIP-seq binding from 2 independent experiments. (C) Genomic location of ZZZ3 (left) and SPT20 (right) ChIP-seq binding in K562 cells. Summary of consensus peaks from 2 independent ChIP-seq experiments is shown. (D) Representative ChIP-seq peak for ZZZ3 target in K562 cells (*RPS7*) and representative ChIP-seq peak for SPT20 target in K562 cells (*HBB*). (E) Publicly available ChIP-seq tracks for H3K9ac (ENCFF257CLC) and ZZZ3 (ENCFF856KCV) in K562 cells at the *RPS7* and *HBB* loci retrieved from the ENCODE project portal (www.encodeproject.org). The *RPS7* and *HBB* loci in panel D are represented confirming the presence of H3K9ac peaks and reproducing the selective ZZZ3 binding at *RPS7* also observed in our data. (F) H3K9ac ChIP-qPCR analysis of representative SPT20 and ZZZ3 targets upon knockdown in K562 cells. N ≥ 3 independent experiments. Mean ± SEM of enrichment relative to rabbit IgG, with normalization to control intergenic region with no significant H3K9ac enrichment. Two-tailed Student *t* test for significance **P* < .05. (G) qRT-PCR analysis of expression of ATAC and SAGA complex targets in K562 cells. N ≥ 3 independent experiments, mean ± SEM of gene expression relative to *CTRLsh*, normalized to *HPRT1* housekeeping gene. Two-tailed Student *t* test for significance **P* < .05, ***P* < .01, ****P* < .001.

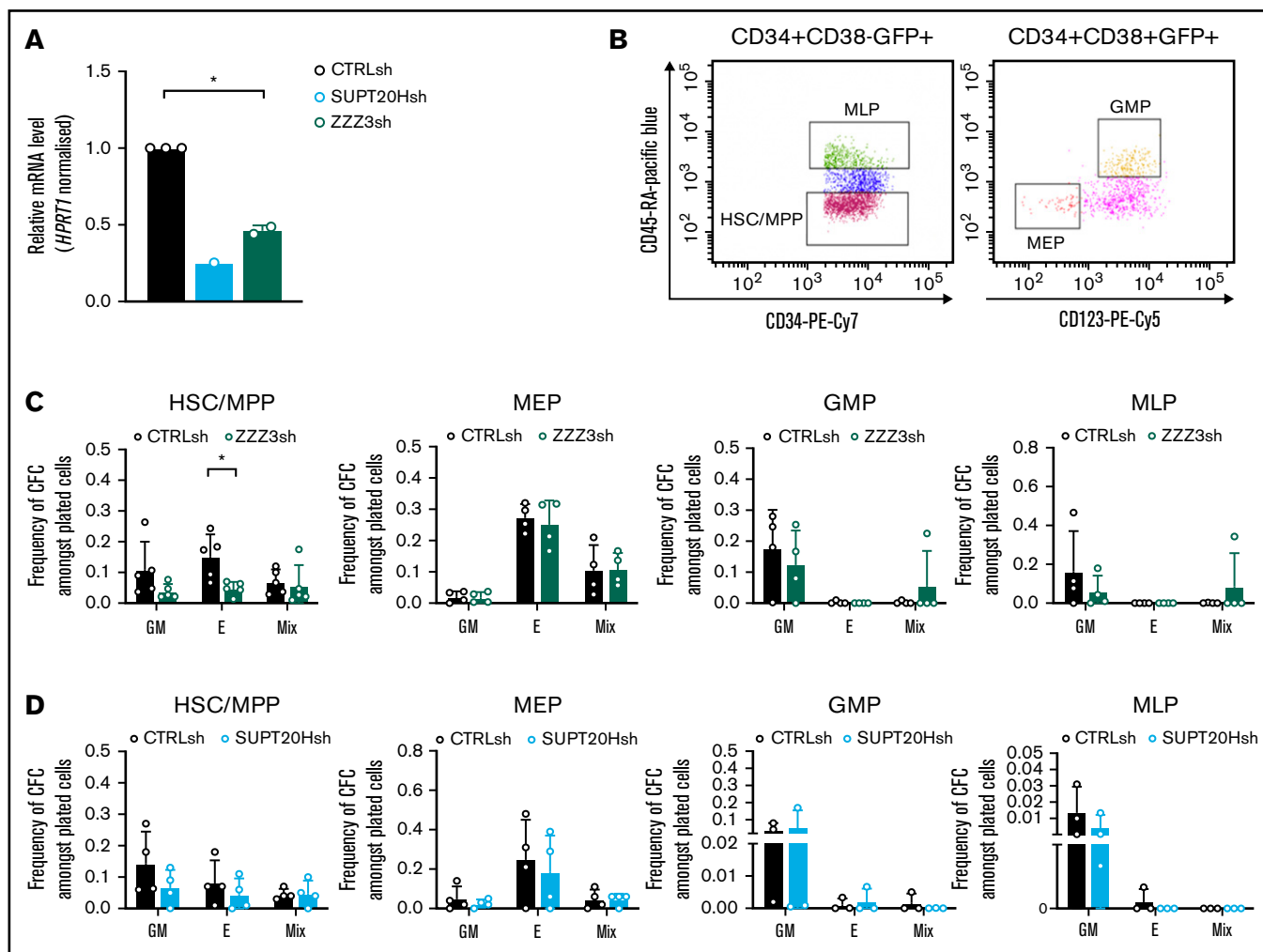


Figure 2. ATAC is selectively required for erythroid specification from CB HSC. (A) qRT-PCR validation of *SUPT20H* and *ZZZ3* knockdown in human CB HSC. Representative experiment for *SUPT20H*; mean \pm SEM of 2 individual experiments for *ZZZ3*; gene expression relative to CTRLsh, normalized to *HPRT1* housekeeping gene. Paired 2-tailed Student *t* test for significance **P* < .05. (B) Representative sorting plot for transduced HSC and progenitor cells from CB. (C) Frequency of CFC efficiency in the HSC/multipotent progenitor (MPP), MEP, GMP, and MLP compartments transduced with *ZZZ3sh*. Mean \pm SEM of 5 individual CB samples (4 for GMP, MLP). Two-tailed paired Student *t* test for significance; **P* < .05. (D) Frequency of CFC efficiency in the HSC/MPP, MEP, GMP, and MLP compartments transduced with *SUPT20Hsh*. Mean \pm SEM of 4 individual CB samples. Two-tailed paired Student *t* test for significance; no significant differences.

medium supplemented with 10% FBS, P/S/A, and L-Gln as above. Cultures were kept at 37°C and 5% CO₂.

Human CB CD34⁺ cells and AML patient samples

Cord blood (CB) samples and AML patient samples were obtained with informed consent under local ethical approval, research ethics committee 07MRE05-44 (Cambridge) and ethics committee code number 94/2016/O/Tess (Bologna). Mononuclear cells (MNC) were isolated by Ficoll-Paque density gradient (StemCell Technologies) centrifugation. CB MNC were enriched for CD34⁺ cells using the RosetteSep Human CB CD34 Pre-Enrichment Cocktail (Stem Cell Technologies) as per manufacturer's instructions.

Lentiviral packaging and transduction

Viral constructs containing control short hairpin RNA (shRNA) (CTRLsh, noneukaryotic gene targeting) or shRNA targeting *KAT2A*

(*KAT2Ash*), *SGF29* (*CCDC101sh*), *SUPT20H* (*SUPT20Hsh* and *SUPT20sh2*), *USP22* (*USP22sh*), *ZZZ3* (*ZZZ3sh*), *TADA2A* (*TADA2Ash* and *TADA2Ash2*), and *TADA2B* (*TADA2Bsh*) (supplemental Table 1) were packaged in HEK 293T cells as previously described,²⁸ using Turbofect (Thermo) or trans-IT (Mirus) as lipofection reagents. Cell lines were transduced overnight with 1-2 T75 packaging flask-equivalents/10⁶ cells and washed the following day as described.²⁸ Green fluorescent protein-positive (GFP⁺) cells were sorted and used in downstream assays 4 days later. CD34⁺ CB cells were prestimulated in serum-free medium (hematopoietic stem cell [HSC] expansion medium XF, Miltenyi Biotec) with stem cell factor (SCF), thrombopoietin (TPO), and Flt3L (respectively 200, 20, and 20 ng/mL) for up to 24 hours and transduced overnight using 2 flask-equivalents/2-3*10⁵ cells. Cells were washed the following day and cultured in half the cytokine concentration for an additional 2 to 3 days prior to sorting.

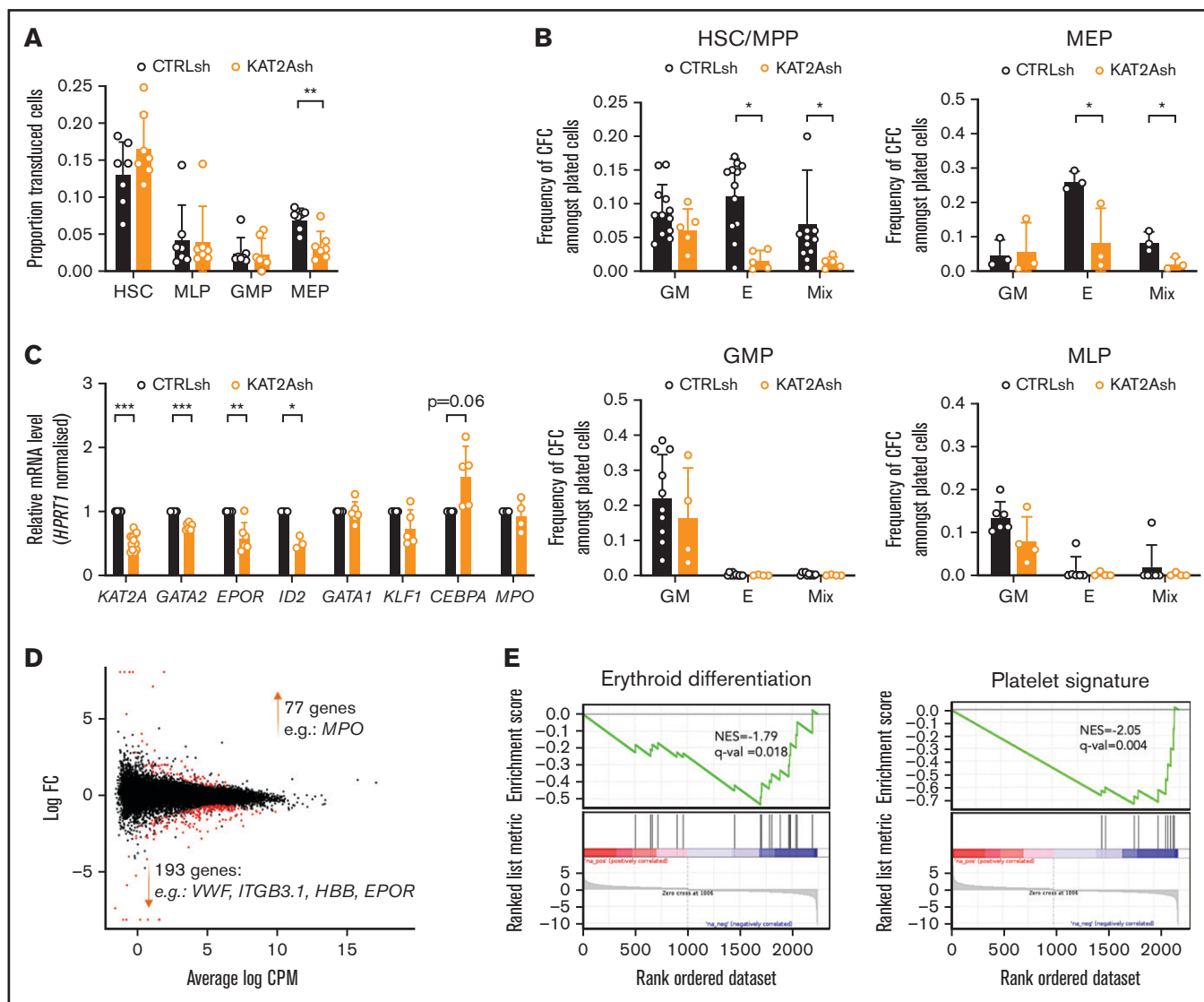


Figure 3. KAT2A regulates human CB erythroid progenitor specification and survival. (A) Proportion of *KAT2A*sh-transduced CB HSC and progenitors. Mean \pm SEM of >7 individual sorting experiments. Two-tailed paired Student *t* test for significance; ***P* < .01. (B) Frequency of CFC efficiency in the HSC/MPP, MEP (top), GMP, and MLP (bottom) compartments transduced with *KAT2A*sh. Mean \pm SEM of 7 individual CB samples. Two-tailed paired Student *t* test for significance; **P* < .05. (C) qRT-PCR analysis of expression of erythroid-associated genes in *KAT2A*sh-transduced HSC from individual CB samples. *N* \geq 3 independent experiments, mean \pm SEM of gene expression relative to *CTRL*sh, normalized to *HPRT1* housekeeping gene. Two-tailed paired Student *t* test for significance **P* < .05, ***P* < .01, ****P* < .001. (D) MA plot of RNA-seq gene expression analysis of differentially-expressed genes (red) in *CTRL*sh vs *KAT2A*sh transduced HSC/MPP cells. (E) Gene set enrichment analysis plot for erythroid differentiation (right) and platelet signature (left) in the RNA-seq data in panel D. Gene signature identifiers are *ADDYA* erythroid differentiation by *HEMIN* and *GNATENKO* platelet signature, respectively, as obtained from the UC San Diego and BROAD Institute Molecular Signatures Database (MSigDB).

Colony-forming cell assays

Sorted CB cells were seeded in methyl-cellulose-based semisolid medium (StemMACS HSC-CFU media complete with erythropoietin [EPO]; Miltenyi Biotec) for assessment of multilineage colony-forming activity. Sorted cells were counted and resuspended in Iscove modified Dulbecco medium 10% FBS supplemented with P/S/A and 2 mM L-Gln prior to addition to the semisolid medium, which was plated in duplicate onto 35 mm dishes with 200 to 300 cells/dish. In the case of colony-forming cell (CFC) assays performed in the presence of the *KAT2A* inhibitor MB-3 (Abcam), this was added to the methylcellulose in a final concentration of

200 μ M and dispersed by vortexing prior to addition of CB cells as described.⁸ Colonies were scored by microscopy at 10 to 12 days at the point of full colony hemoglobinization.

Mixed lineage differentiation cultures

CB CD34⁺ cells were cultured for up to 7 days in serum-free liquid culture (StemSpan, Stem Cell Technologies) in the presence of SCF, Flt3-L, IL-3, IL-6 (1x CC100; Stem Cell Technologies), and EPO 3 U/ μ L (R&D). Transduced CD34⁺/HSC were seeded as GFP⁺ cells immediately after sorting. In other experiments, enriched CD34⁺ cells were resuspended in serum-free medium

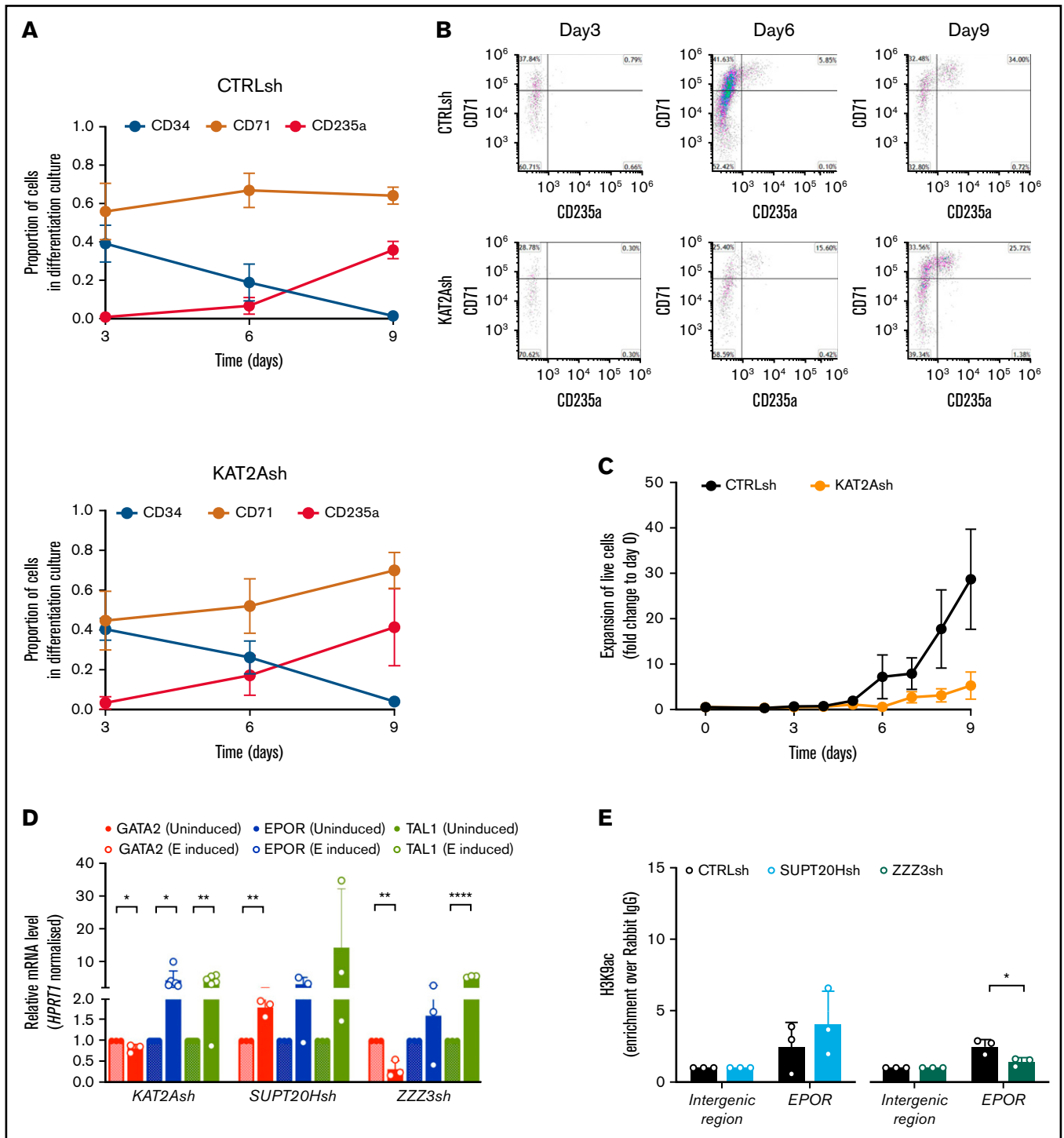


Figure 4. KAT2A SAGA and ATAC complexes differentially affect erythroid lineage progression. (A) Erythroid differentiation of HSC/MPP sorted from CD34⁺ cells of individual CB samples transduced with *CTRLsh* (top) and *KAT2Ash* (bottom) in liquid cultures. CD34 marks HSC and progenitors; CD71 and CD235a mark early and late differentiated erythroid cells. Data summarize mean \pm SEM of 4 independent differentiation experiments. (B) Flow cytometry quantitative analysis of *CTRLsh* and *KAT2Ash* HSC in erythroid differentiation cultures in panel A. Representative plots. (C) Expansion of *CTRLsh* and *KAT2Ash* HSC in erythroid differentiation cultures in panel A. (D) qRT-PCR analysis of erythroid gene expression progression in K562 cells transduced with *KAT2Ash*, *SUPT20Hsh*, or *ZZZ3sh* and treated with 1.5% DMSO for erythroid molecular induction. Mean \pm SD of $n > 3$ independent experiments; data are represented relative to day 0 normalized to *HPRT1* housekeeping gene. Two-tailed paired Student *t* test for significance **P* < .05, ***P* < .01, *****P* < .0001. *CTRLsh*-transduced cells for the same experiment shown in supplemental Figure 4C. (E) H3K9ac ChIP-qPCR analysis of *EPOR* locus in K562 cells upon *SUPT20H* and *ZZZ3* knockdown. $N \geq 3$ independent experiments. Mean \pm SEM of enrichment relative to rabbit IgG, with normalization to control intergenic region with no significant H3K9ac enrichment. Two-tailed Student *t* test for significance **P* < .05.

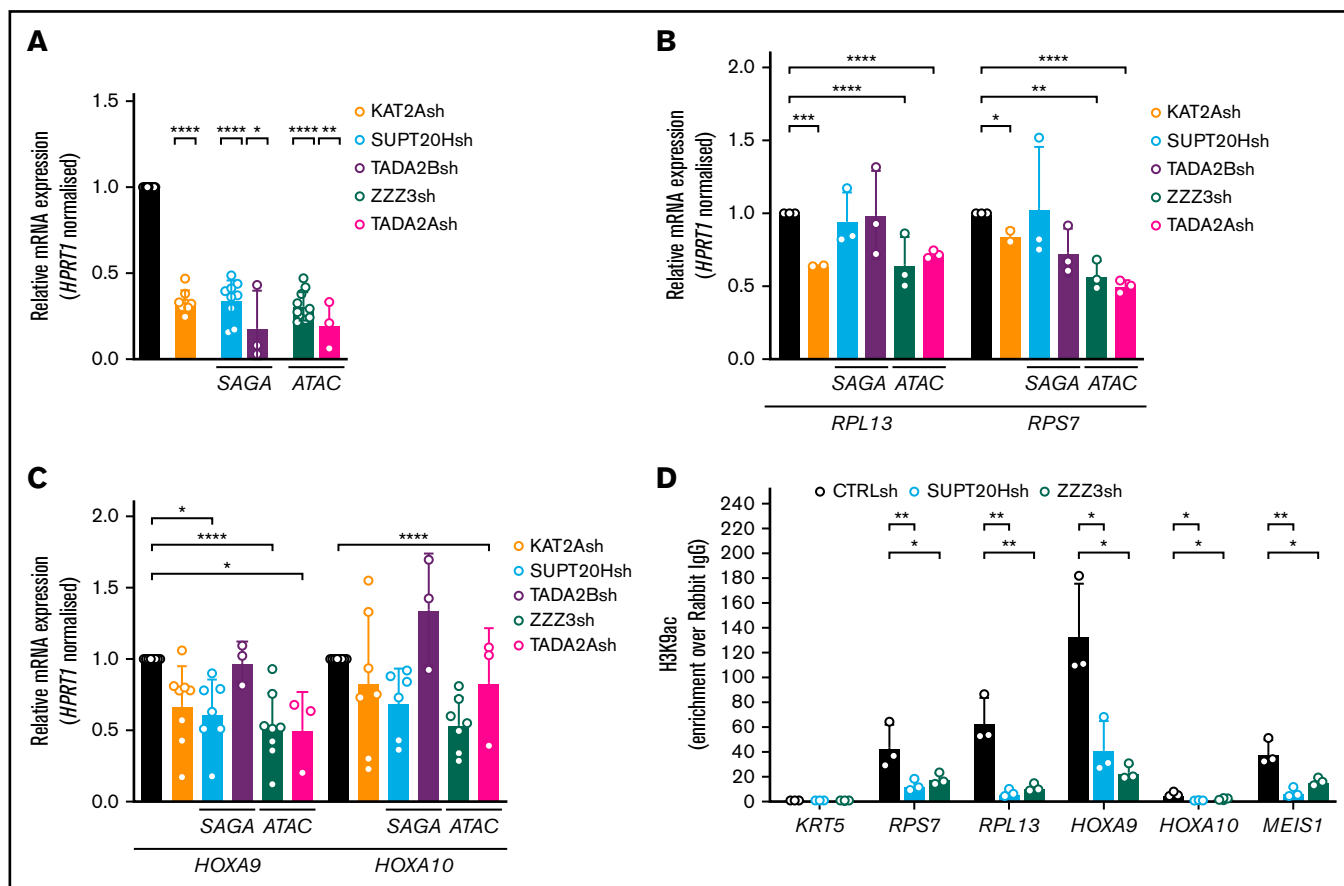


Figure 5. ATAC and SAGA differentially impact histone acetylation and gene expression in MOLM13 AML cells. (A) qRT-PCR validation of *KAT2A*, *SUPT20H*, *TADA2B* (SAGA-specific subunits), *ZZZ3*, and *TADA2A* (ATAC-specific subunits) knockdown in MOLM-13 cells. $N \geq 3$ independent experiments, mean \pm SEM of gene expression relative to *CTRLsh*, normalized to *HPRT1* housekeeping gene. Two-tailed Student *t* test for significance * $P < .05$, ** $P < .01$, **** $P < .0001$. (B) qRT-PCR analysis of ribosomal protein gene expression in MOLM-13 cells transduced with *KAT2Ash*, SAGA-specific *SUPT20Hsh* and *TADA2Bsh*, and ATAC-specific *ZZZ3sh* and *TADA2Ash*. $N \geq 3$ independent experiments, mean \pm SEM of gene expression relative to *CTRLsh*, normalized to *HPRT1* housekeeping gene. Two-tailed Student *t* test for significance * $P < .05$, ** $P < .01$, *** $P < .001$, **** $P < .0001$. (C) qRT-PCR analysis of self-renewal gene signature in MOLM-13 transduced with *KAT2Ash*, SAGA-specific *SUPT20Hsh* and *TADA2Bsh*, and ATAC-specific *ZZZ3sh* and *TADA2Ash*. $N = 2$ biological replicates, each run as 2 or 3 technical repeats; mean \pm SEM of relative gene expression relative to *CTRLsh*, normalized to *HPRT1* housekeeping gene. Two-tailed nested Student *t* test for significance * $P < .05$, **** $P < .0001$. (D) H3K9ac ChIP-qPCR analysis of ribosomal protein genes and self-renewal genes in MOLM-13 cells upon knockdown of SAGA and ATAC elements *SUPT20H* and *ZZZ3*, respectively. $N \geq 3$ independent experiments. Mean \pm SEM of enrichment relative to rabbit IgG, with normalization to control region in *KRT5* locus with no significant H3K9ac enrichment. Two-tailed Student *t* test for significance * $P < .05$, ** $P < .01$.

and cytokines in the presence of MB-3 (Abcam) 100 μ M. Fresh cytokines, and, where appropriate, inhibitor and vehicle DMSO, were added every 2 to 3 days. At different time points, cells were tested by flow cytometry for the presence of CD34, CD13, and CD71/CD235a surface markers.

Erythroid differentiation and induction cultures

Transduced HSC were tested in erythroid differentiation conditions in serum-free liquid culture (HSC expansion medium xeno-free; Miltenyi Biotec) in the presence of hydrocortisone (10^{-5} M), SCF (100 ng/mL), TPO (10 ng/mL), and EPO (3 U/mL). Cultures were followed up for 9 days with daily live and dead cell counts and regular flow cytometry analysis for CD34, CD71, and CD235a markers (supplemental Table 4). K562 cells were induced to the erythroid lineage in the presence of 1.5% DMSO as described.²⁹ Cells were monitored for differentiation markers (CD71 and CD235a) and/or

activation of erythroid-affiliated molecular programs during a 6-day culture period.

AML-MS5 coculture

MS5 murine bone marrow stromal cells were grown in Iscove modified Dulbecco medium supplemented with 10% FBS, 1% P/S/A, and 2 mM L-Gln. Cells were subcultured twice a week and passage 2 was used to carry out experiments in 48-well plates. AML cells were thawed in PBS 2% FBS, 1% P/S/A, and prestimulated with H5100 (Stem Cell Technologies) supplemented with IL-3 20 ng/mL, G-CSF 20 ng/mL, and TPO 20 ng/mL (3GT), 1% *N*-2-hydroxyethylpiperazine-*N'*-2-ethanesulfonic acid, and 1% P/S/A for \sim 4 hours. Cells were then transduced with the desired lentiviral constructs in transduction media: H5100 with SCF (100 ng/mL), Flt-3 (100 ng/mL), IL-3 (60 ng/mL), TPO (10 ng/mL), 1% *N*-2-hydroxyethylpiperazine-*N'*-2-ethanesulfonic acid, and 1% P/S/A. Cells were

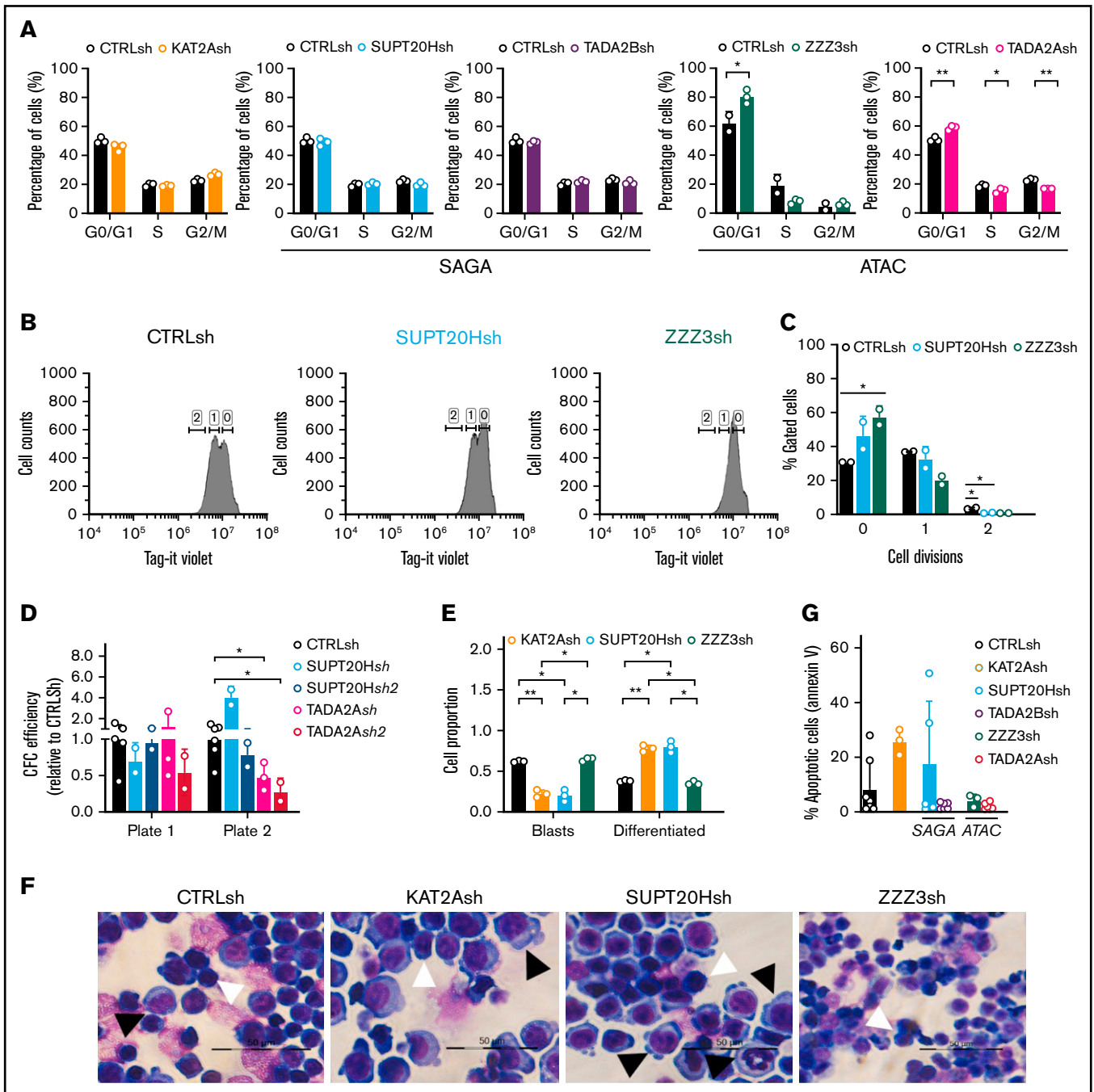


Figure 6. ATAC maintains self-propagation and SAGA blocks differentiation of MOLM13 AML cells. (A) Quantification of flow cytometry analysis of cell cycle in MOLM-13 cells transduced with *KAT2Ash*, SAGA-specific *SUPT20Hsh* and *TADA2Bsh*, and ATAC-specific *ZZZ3sh* and *TADA2Ash*. Corresponding representative plots in supplemental Figure 5C. Mean \pm SEM of 3 independent experiments. Two-tailed Student *t* test for significance **P* < .05, ***P* < .01. (B) Representative flow cytometry plots of divisional tracking of MOLM-13 cells transduced with *CTRLsh*, *SUPT20Hsh*, and *ZZZ3sh* and loaded with the Tag-IT violet dye (Biologend) after 3 days of culture. Regions 0, 1, and 2 represent the number of cell divisions relative to initial loading control (also see supplemental Figure 5D-E). (C) Quantification of results in panel B representing the distribution of MOLM-13 cells transduced with *CTRLsh*, *SUPT20Hsh*, and *ZZZ3sh* undergone 0-2 cell divisions after 3 days in culture. Mean \pm SEM of 3 independent experiments. Two-tailed Student *t* test for significance **P* < .05. (D) Colony replating of MOLM-13 cells transduced with *SUPT20Hsh1*, *SUPT20Hsh2* (SAGA), *TADA2Ash1*, and *TADA2Ash2* (ATAC) as a measure of in vitro self-renewal. Mean \pm SEM of 2-3 independent experiments. Two-tailed Student *t* test for significance **P* < .05. (E) Quantification of blast-like and differentiated cells in MOLM-13 cultures transduced with *CTRLsh*, *KAT2Ash*, *SUPT20Hsh*, and *ZZZ3sh*. Scoring of 3 randomly selected fields of >100 cells; Two-tailed Student *t* test for significance; **P* < .05, ***P* < .01. (F) Representative photographs of MOLM-13 cytopins. White arrow heads denote blast-like cells; black arrow heads denote differentiated cells. Bar represents 50 μ m. (G) Quantification of Annexin V⁺ apoptotic cells in MOLM13 cultures analyzed by flow cytometry (representative plots in supplemental Figure 4F). Mean \pm SEM of n > 3 independent experiments. Two-tailed Student *t* test for significance.

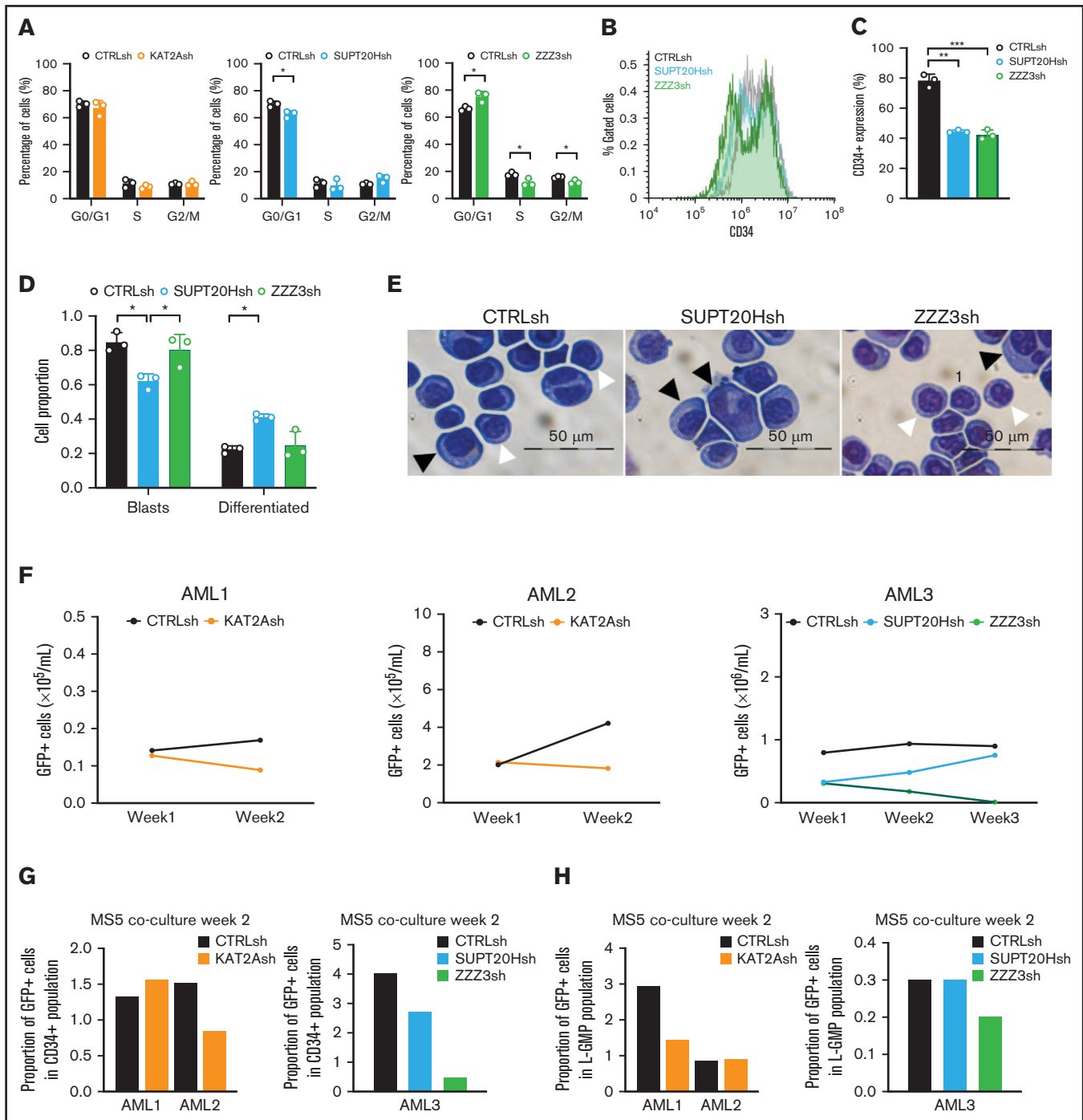


Figure 7. KAT2A complex activity maintains propagation of undifferentiated cultured and primary CD34⁺ AML cells. (A) Quantification of flow cytometry analysis of cell cycle in Kasumi-1 cells transduced with *KAT2Ash*, *SUPT20Hsh*, and *ZZZ3sh*. Mean \pm SEM of 3 independent experiments. Two-tailed Student *t* test for significance $*P < .05$. (B) Representative flow cytometry overlay plot of analysis of undifferentiated marker CD34 in KG1a cells transduced with *CTRLsh*, *SUPT20Hsh*, and *ZZZ3sh*. (C) Quantification of CD34⁺ cells in transduced KG1a cells in panel B. N = 3 independent experiments. Two-tailed Student *t* test for significance $**P < .01$. (D) Quantification of blast-like and differentiated cells in KG1a cultures transduced with *CTRLsh*, *SUPT20Hsh*, and *ZZZ3sh*. Scoring of 3 randomly selected fields of >100 cells; Two-tailed Student *t* test for significance; $*P < .05$. (E) Representative photographs of KG1a cytopsin. White arrow heads denote blast-like cells; black arrow heads denote differentiated cells. Bar represents 50 μ m. (F) Growth of human primary AML cells (CD34⁺ samples; details in supplemental File 5) transduced with *CTRLsh*, *KAT2Ash*, *SUPT20Hsh*, or *ZZZ3sh* and maintained in the MS5 coculture system for 2-3 weeks. (G) Percentage of GFP⁺ CD34⁺ cells in AML samples in panel F analyzed at week 2 of the MS5 coculture. Analysis gates are presented in supplemental Figure 6A. Data are normalized to global GFP level to correct for unequal GFP transduction levels. (H) Percentage of GFP⁺ GMP-like (L-GMP) cells at week 2 of the MS5 coculture system in AML samples in panel F. Analysis gates in supplemental Figure 7A. GFP transduction correction as in panel G.

washed twice in PBS 2% FBS and 1% P/S/A, once in H5100 1% P/S/A, and seeded onto MS5 stroma. Cultures were kept at 37°C and 5% CO₂ for up to 3 weeks, with twice-weekly demipopulation and fresh addition of H5100-3GT. For KAT2A inhibition experiments, AML MNC were seeded onto MS-5 stroma in H5100-3GT in the presence of 100 μM of MB-3 (Abcam) or DMSO (0.1%) and demipopulated as above with fresh addition of MB-3. Cells were stained for flow cytometry analysis once a week (supplemental Table 4).

Chromatin immunoprecipitation

For chromatin immunoprecipitation (ChIP)-sequencing (ChIP-seq), chromatin was prepared in duplicate from K562 cells (9 sonication cycles, 30"ON/30"OFF) and immunoprecipitated using anti-SPT20 and anti-ZZZ3 sera prepared in the Tora Laboratory.¹³ All procedures, including library preparation and sequencing, were performed as described.⁷ For ChIP-quantitative polymerase chain reaction (qPCR), K562 cells were immunoprecipitated with anti-H3K9ac antibody or rabbit immunoglobulin G (IgG) (supplemental Table 2); eluted DNA was diluted and quantified by SYBR green qPCR using 2 μL DNA per triplicate reaction (primers in supplemental Table 3). Peak enrichments relative to rabbit IgG were determined using the 2^{ΔΔC_t} method with a reference intergenic region or *KRT5*.

Statistical analysis

Statistical analysis was performed in GraphPad Prism 7 software (GraphPad Software). Data are reported as mean ± standard error of the mean (SEM). Significance calculated by 2-tailed Student *t* test at *P* < .05 (see individual figure legends for details).

Results

KAT2A-containing ATAC and SAGA complexes have unique targets in hematopoietic cells

In order to identify unique ATAC and SAGA targets and characterize complex-specific roles of KAT2A in the blood system, we performed ChIP followed by next-generation sequencing (ChIP-seq) of ZZZ3 (ATAC-specific) and SPT20 (SAGA-specific) subunits (Figure 1A) in human K562 cells. K562 are a chronic myelogenous leukemia cell line with multilineage potential: cells display aspects of molecular differentiation into erythroid, megakaryocytic, and macrophage identities under defined cytokine conditions²⁹; in steady state, K562 cells represent immature leukemia blasts with self-renewal properties. K562 cells have been previously used as a model for understanding molecular mechanisms of normal, particularly erythroid, and malignant blood specification.³⁰⁻³³ We made use of specific sera against human ZZZ3 and SPT20 and performed ChIP-seq experiments in duplicate in self-renewing K562 cells. As in previous reports,¹³ we found limited overlap between ATAC and SAGA targets (Figure 1B; supplemental File 1). Bound peaks were preferentially found in the vicinity of the transcriptional start site (Figure 1C) and were robustly enriched for ZZZ3 and SPT20 experimental targets, respectively (supplemental Figure 1A-B), as cataloged in the ENCODE database.³⁴ ZZZ3 peaks were more proximal than SPT20's, in contrast with previously described enhancer association of ATAC complexes in lymphoblast and HeLa cells.¹³ Our results are nevertheless consistent with a distinct ZZZ3 ChIP-seq experiment in human non-small cell lung cancer cells, which revealed strong enrichment of ZZZ3 peaks in regions ±1 kb of the

transcriptional start site.²¹ This suggests that ATAC-complex enhancer region occupancy may be cell type or context-dependent. Interrogation of functional associations of ZZZ3 and SPT20 peaks highlighted complex-specific biologies (supplemental Figure 1C-D). These are reflected in distinct gene ontology categories associated with complex-specific peaks, which encompass RNA and ribosomal metabolism in the case of ATAC (Figure 1D; supplemental Figure 1C) and transcriptional activity for SAGA (supplemental Figure 1D). Moreover, SAGA specifically binds red blood cell-associated genes (Figure 1D), which may indicate a unique role in erythroid differentiation or identity. Inspection of publicly available K562 ChIP-seq datasets in the ENCODE database confirmed that SPT20 and ZZZ3-bound regions coincided with H3K9ac peaks, a hallmark of KAT2A enzymatic activity (Figure 1E).⁹ By making use of lentiviral-delivered shRNA targeting SPT20 or ZZZ3, we verified that selected SAGA and ATAC ChIP-seq target loci did indeed reduce promoter H3K9ac (Figure 1F) upon *SUPT20H* and *ZZZ3* knockdown (Figure 1G; supplemental Figure 1E), respectively. The same target loci had reduced gene expression upon *SUPT20H* or *ZZZ3* loss, suggesting that the chromatin binding had activating consequences for gene expression in a complex-specific manner (Figure 1G). Observed gene expression changes could be partially recapitulated upon *KAT2A* gene expression knockdown (supplemental Figure 1F-G), particularly in respect of ZZZ3-bound elements, which could reflect differential dependence and/or redundancy of histone acetyltransferase activity in either complex. Indeed, K562 cells were more clearly dependent on ZZZ3 than on SPT20 for propagation in culture (supplemental Figure 1H). Loss of *KAT2A* had an intermediate effect (supplemental Figure 1H), in line with independent activities of each complex in hematopoietic cell maintenance and/or identity, which might be balanced by the action of *KAT2A*.

We have recently established a role for *KAT2A*^{7,8} in maintenance of AML cells, which could be akin to our observations in K562 cells. In contrast, we and others failed to identify a specific requirement for *Kat2a* in normal mouse hematopoiesis,^{6,7} which contrasts with SAGA SPT20 chromatin binding of erythroid lineage loci. We therefore sought to systematically dissect SAGA and ATAC-mediated *KAT2A* contributions to normal and myeloid leukemic hematopoiesis in primary and cultured human cells.

ATAC is selectively required for erythroid specification from CB HSC

We started by inspecting putative differential functional contributions of SAGA and ATAC complexes to normal human hematopoiesis by transducing CD34⁺ CB cells with lentiviral-delivered ZZZ3 or *SUPT20H* shRNAs (Figure 2A). We flow-sorted transduced (GFP⁺) CD34⁺ cells as stem and multipotent progenitor cells (HSC) or as lineage-restricted myelo-lymphoid (MLP), megakaryocytic-erythroid (MEP), and granulocytic-monocytic progenitors (GMP) (Figure 2B) and assessed their cell differentiation and proliferation potential in CFC progenitor assays (supplemental Figure 2A). We did not observe differences in the stem and progenitor proportions of transduced cells with either construct (supplemental Figure 2B-C). In contrast, CFC assay output revealed a unique defect in erythroid specification from HSC upon ZZZ3 loss (Figure 2C), with no changes to generation of mixed-lineage or GM colonies. Colony formation from downstream lineage-restricted progenitors was not affected, suggesting a

unique requirement for *ZZZ3* in early erythroid commitment and a dispensable role for the ATAC component posterythroid commitment, as well as in the myelo-monocytic lineages. *SUPT20H* expression knockdown, on the other hand, did not result in changes in colony-forming efficiency from either HSC or lineage-restricted progenitors (Figure 2D). However, knockdown of the deubiquitinase component of the SAGA complex, *USP22* (supplemental Figure 2D-E), resulted in loss of erythroid colony formation from committed MEP (supplemental Figure 2F), which did not significantly affect pre-commitment HSC and multipotent progenitors (supplemental Figure 2F). In agreement, proportions of $CD34^+$ progenitors were unaffected (supplemental Figure 2G). Taken together, the data support contrasting roles for the ATAC and SAGA complexes in normal human blood progenitor biology, with early erythroid lineage specification dependent on *ZZZ3*. SAGA elements, in turn, participate in the development of the erythroid lineage postcommitment as suggested by gene regulation in K562 cells, although their requirement may be less absolute.

KAT2A regulates human CB erythroid progenitor specification and survival

Given the differential role of ATAC and SAGA elements in the erythroid lineage, we asked if *KAT2A* itself was required in human CB progenitor specification or differentiation. To reiterate, chemical inhibition of *KAT2A* activity at the 100 μ M dose effective in AML cell lines had not resulted in an overall reduction in colony formation from CB $CD34^+$ cells,⁸ and we and others had not found a requirement for *Kat2a* in mouse bone marrow hematopoiesis.^{1,2} Nevertheless, reinspection of *Kat2a* expression in bone marrow subpopulations of our conditional knockout model⁷ revealed that gene expression ablation in MEP was less extensive than in myelomonocytic cells ($n = 4$; mean \pm standard deviation: 0.39 ± 0.20 in MEP vs 0.13 ± 0.08 in GMP, 2-tailed Student *t* test; $P = .054$), compatible with selective preservation of unexcised *Kat2a* allele-carrying MEP cells and a possible partial requirement for *Kat2a* expression. In agreement, transduction of CB $CD34^+$ cells with *KAT2A* *shRNA* resulted in a significant and specific proportional decrease in *KAT2A*-depleted MEP (Figure 3A), suggesting a defect in specification of CB progenitors committed to the erythroid lineage. Inspection of progenitor activity of CB $CD34^+$ cells in CFC assays upon *KAT2A* knockdown (supplemental Figure 3A) or chemical inhibition (supplemental Figure 3B) detected a reduction in erythroid colony formation. The same reduction was observed upon depletion of the Tudor domain protein SGF29 (gene *CCDC101*) (supplemental Figure 3C-D), a *KAT2A* partner common to SAGA and ATAC complexes. Equally, culture of *KAT2A* knockdown (supplemental Figure 3E) or MB-3 inhibited (supplemental Figure 3F) $CD34^+$ cells in mixed-lineage differentiation conditions resulted in relative loss of differentiated erythroid cells, compatible with hindered specification of the red blood cell lineage. Dissection of HSC and progenitor $CD34^+$ compartments revealed that loss of *KAT2A* affected erythroid lineage output from both HSC and MEP (Figure 3B) without changes to myelo-monocytic lineage output (Figure 3B), thus capturing both ATAC and SAGA-associated effects. Quantitative reverse transcription polymerase chain reaction (qRT-PCR) transcriptional analysis of *KAT2A* knockdown HSC shows downregulation of early erythroid regulatory genes, namely *GATA2* and *EPOR*, (Figure 3C), a finding compatible with the global reduction of erythroid and megakaryocytic programs

apparent upon RNA-seq analysis (Figure 3D-E; supplemental File 2). Analysis of effects of *KAT2A* knockdown on cell cycle and apoptosis is suggestive of putative effects on cell survival perierythroid commitment (supplemental Figure 3G-H), with specific increases in apoptotic HSC and MEP, which do not extend to other lineages. Taken together, the data support a function for *KAT2A* in specification and/or survival of erythroid-megakaryocytic progenitors.

SAGA facilitates progression of erythroid differentiation

Colony-forming progenitor assays of CB $CD34^+$ cells associated with loss of *KAT2A*-containing ATAC complexes with impairment of early erythroid and megakaryocytic specification (Figure 2C). The data also suggested that *KAT2A*-containing SAGA complexes may play a role in erythroid differentiation postcommitment (supplemental Figure 2F). However, CFC assays are end-point assays that do not permit a detailed dissection of mechanisms of differentiation, and we attempted to overcome this limitation using a liquid culture system. Differentiation of total CB $CD34^+$ cells in the presence of hydrocortisone, SCF, TPO, and EPO resulted in progressive loss of $CD34$ and accumulation of glycophorin A (*CD235a*)-positive cells, denoting effective erythroid differentiation (Figure 4A), which was not qualitatively impaired upon *KAT2A* knockdown (Figure 4B). However, erythroid differentiation cultures initiated from *KAT2A*-depleted HSC were quantitatively impaired, being severely restricted in their expansion (Figure 4C). Reduced *KAT2A* knockdown cell growth was accompanied by a general trend toward increased cell death (supplemental Figure 4A), compatible with the observed *KAT2A* role in HSC and MEP cell survival. To circumvent the limiting cell numbers in transduced primary CB cultures, we inspected erythroid lineage progression and associated molecular programs in K562 cells. Exposure of K562 cells to 1.5% DMSO resulted in accumulation of $CD235a^+$ cells and progressive loss of the earlier $CD71$ transferrin receptor (supplemental Figure 4B) and was accompanied by loss of *GATA2* and upregulation of *EPOR* and *TAL1*, denoting molecular erythroid lineage progression²⁹ (supplemental Figure 4C). DMSO-induced erythroid cultures initiated by *KAT2A* knockdown cells followed a similar molecular progression (Figure 4D). In contrast, *SUPT20H* depletion significantly perturbed induction of erythroid programs in K562 cells, which failed to downregulate *GATA2*, and variably upregulated *EPOR* and *TAL1*, suggestive of a defect in lineage progression (Figure 4D). We confirmed the findings with a second *SUPT20H* *shRNA* (*SUPT20Hsh2*) (supplemental Figure 4D-F). Accordingly, inspection of the expression pattern of SAGA-specific elements during *in vitro* maturation of committed erythroid progenitors from human CB³⁵ showed that several elements associate with late differentiation (supplemental Figure 4G), including members of the core, the SAGA-specific HAT subunit *TADA2B*, and the H2B deubiquitinase *USP22* (supplemental File 3), which specifically affected erythroid colony formation from MEP in human CB. In contrast, inspection of the detailed single-cell profiling of erythroid development by Tusi et al³⁶ captured *Kat2a* and *Zzz3* enrichment, but no elements of the SAGA complex, at the transition of multipotent progenitors to the erythroid and megakaryocytic lineages (supplemental Figure 4H; supplemental File 4), compatible with an early specification role of ATAC that does not extend into terminal erythroid differentiation. Indeed, loss of *ZZZ3* allowed downregulation of *GATA2* and

upregulation of *TAL1* during K562 erythroid induction (Figure 4D). However, *EPOR* was not consistently upregulated (Figure 4D), a trend confirmed upon knockdown of a second ATAC element, *TADA2A* (supplemental Figure 4E), which resulted in minimal *EPOR* upregulation, which was significantly lower than that observed for *CTRLsh* (1.52 ± 0.13 *TADA2Ash* vs 3.19 ± 0.49 *CTRLsh* fold change relative to undifferentiated cells; $P = .0214$). Inspection of the K562 ZZZ3 ChIP-seq data showed binding of the *EPOR* locus in one of the 2 replicate samples (supplemental File 1; supplemental Figure 4I), and we checked if ZZZ3 knockdown resulted in loss of H3K9ac at the *EPOR* promoter. Indeed, we observed that ZZZ3, but not *SUPT20H* loss, decreased *EPOR* H3K9 acetylation (Figure 4E), suggesting that *KAT2A* requirement for early erythroid specification may be mediated by ATAC control of *EPOR* expression and downstream signaling. However, we could not detect consistent downregulation of *EPOR* in steady-state K562 cells upon ZZZ3 or *TADA2A* knockdown (supplemental Figure 4J), suggesting that regulation of *EPOR* by ATAC may be context-dependent and not an absolute requirement for *KAT2A*-mediated regulation of early erythroid specification or survival.

In conclusion, our analysis of normal erythroid lineage progression indicates that *KAT2A* plays stage-specific roles, which differentially align with each of the 2 complexes it integrates. On the one hand, *KAT2A* regulates specification and survival of erythroid progenitors through participation in the ATAC complex, which controls biosynthetic activity, and to some extent, *EPOR* expression. On the other hand, *KAT2A* fine-tunes progression of erythroid lineage programs through participation in SAGA, which is only required in fully-committed progenitors and may play a contributory rather than an absolute role. Notably, *SUPT20H* regulation of erythroid molecular progression in K562 cells exceeds the contribution of *KAT2A* itself. It is possible that SAGA complexes also use the ortholog histone acetyltransferase *KAT2B* in this context, which can compensate for *KAT2A* loss. Increased *KAT2B* expression in progressed erythroid differentiation, accompanying upregulation of SAGA elements (supplemental File 3), is compatible with this view.

KAT2A complexes uniquely maintain proliferation and identity of MOLM13 AML cells

Having demonstrated that *KAT2A*-containing ATAC and SAGA complexes differentially sustain early lineage establishment and differentiation of erythroid progenitor cells from human CB, we asked whether they also made specific contributions to AML biology. We started by investigating the model AML cell line MOLM13, which we had previously shown to be dependent on *KAT2A* expression and activity.⁸ We knocked down expression of ATAC elements ZZZ3 and *TADA2A* and of SAGA components *SUPT20H* and *TADA2B* (Figure 5A), all of which, like *KAT2A* depletion, impacted expansion of MOLM13 cultures (supplemental Figure 5A-B). At a molecular level, depletion of ATAC, but not SAGA elements, impacted expression of ribosomal protein genes (Figure 5B), in line with a pervasive control of protein biosynthetic activity by the ATAC complex, which we observed in K562 cells and others also reported in lung cancer cell lines depleted of ZZZ3 and *YEATS2* expression.^{21,37} Analysis of expression of self-renewal signature genes *HOXA9* and *HOXA10* showed a more extensive association with ATAC elements (Figure 5C). Interestingly, despite the selective impact of ATAC elements on gene expression, loss of both *SUPT20H* and ZZZ3 resulted in depletion of H3K9ac in the

respective ribosomal protein and *HOX* gene promoters (Figure 5D), suggesting that locus regulation may be more complex than the promoter binding observed in K562 cells. Loss of *KAT2A* itself affects ribosomal protein gene expression but not *HOXA* genes (Figure 5B-C). This recapitulates our MLL-AF9 *Kat2a* knockout leukemia mouse model⁷ in which progressive depletion of leukemia stem-like cells does not seem dependent on the classical *Hoxa* signature. Despite some ambiguity at a molecular level, ATAC and SAGA complexes do make a distinct cellular impact on the biology of MOLM-13 cells. Loss of ATAC ZZZ3 and *TADA2A* arrest cell cycle progression in G0/G1 (Figure 6A; supplemental Figure 5C). The proliferation defect is reflected by a reduced number of ZZZ3 knockdown cells entering cell division (Figure 6B-C) over a 3-day culture period (supplemental Figure 5D) as captured by divisional tracking (supplemental Figure 5E). We asked if the proliferation defect consequent to ATAC loss affected MOLM13 cell self-renewal as measured by in vitro replating of CFC assays. Indeed, although neither ATAC (*TADA2A*) nor SAGA (*SUPT20H*) knockdowns impacted initial colony formation, ATAC alone affected replating of colony assays (Figure 6D; supplemental Figure 5F), suggesting an effect on self-renewal. In contrast, loss of SAGA *SUPT20H* resulted in extensive differentiation of MOLM13 cells (Figure 6E-F; supplemental Figure 5G), suggesting a role in preservation of cell identity, which is not unlike SAGA contribution to the development of human erythroid cells. Despite a trend toward enhanced apoptosis of *KAT2A* knockdown cells (Figure 6G; supplemental Figure 5H), which could be an end-point consequence of enhanced differentiation (Figure 6E-F; supplemental Figure 5G), we did not observe a consistent apoptotic response to knockdown of SAGA (*SUPT20H* and *TADA2B*) or indeed ATAC (ZZZ3 and *TADA2A*) elements (Figure 6G; supplemental Figure 5H), suggesting that control of cell survival is not central to *KAT2A* complex-mediated maintenance of MOLM13 AML cells.

Overall, the data support distinct roles for ATAC and SAGA in the model AML cell line MOLM13. ATAC controls biosynthetic activity and impacts self-renewal of MOLM13 cells through molecular control of *HOXA* genes and regulation of cell division. SAGA, on the other hand, preserves cell identity and impedes differentiation. The dichotomy of effects captures different aspects of *KAT2A* regulation of MOLM13 cells and *MLL-AF9*-driven leukemia⁷ and broadly aligns with differential participation of *KAT2A* complexes in normal hematopoiesis.

KAT2A-containing SAGA and ATAC complexes regulate cultured and primary CD34⁺ AML cells

Finally, we sought to extend our analysis of AML cells to include CD34⁺ lines not originally covered by the screen that established *KAT2A* as a critical regulator of AML cells.⁸ Similarly, we investigated primary CD34⁺ AML patient samples for which stem-like compartments have been more clearly established.³⁸ We initially focused on the CD34⁺ AML cell lines KG1a and Kasumi1, both of which represent minimally differentiated AML French-American-British M1 and M2, respectively, and carry distinct molecular abnormalities (KG1a, *FGFR1OP2-FGFR1* fusion; Kasumi1, *RUNX1-RUNX1T1* fusion) representative of human disease.^{39,40} In both models, loss of ATAC, but not SAGA elements, restricted cell cycle progression (Figure 7A; supplemental Figure 6A). Similar to what had been observed in MOLM13 cells, none of the cell lines displayed increased apoptosis in response to loss of *KAT2A*

complexes (supplemental Figure 6B-C). We investigated differentiation consequences of loss of ATAC or SAGA components in KG1a cells and observed downregulation of the CD34 marker by flow cytometry upon *ZZZ3* and *SUPT20H* loss (Figure 7B-C). However, only *SUPT20H* knockdown resulted in morphological differentiation along the monocytic lineage (Figure 7D-E), supporting the notion that the undifferentiated state of AML cells is sustained through SAGA activity. Finally, we attempted to transduce primary CD34⁺ AML patient blasts (supplemental Table 5) with our lentiviral vectors delivering shRNAs against *KAT2A*, *SUPT20H*, or *ZZZ3*. We could observe transduced GFP⁺ cells in <50% of the samples transduced and kept the cells in culture for 2-3 weeks in the presence of MS5 stroma as described,⁴¹ following up their expansion as well as the preservation of CD34⁺ and candidate phenotypic leukemia stem-like (L-)GMP (supplemental Figure 7A). Downregulation of *KAT2A* and *ZZZ3*, but in the sample analyzed, not of *SUPT20H*, resulted in reduced expansion of transduced AML cells (Figure 7F), which specifically affected CD34⁺ (Figure 7G) and/or L-GMP (Figure 7H), suggesting a loss of self-renewal potential. Chemical inhibition of *KAT2A* activity using MB-3⁸ had a similar effect on the preservation of CD34⁺ cells (supplemental Figure 7B), which impacted the proportion of L-GMP (supplemental Figure 7C).

Thus, the data suggest that *KAT2A*-containing complexes, particularly ATAC, play a role in the maintenance of candidate leukemia self-renewing CD34⁺ cells, with SAGA putatively contributing to the AML differentiation block.

Discussion

In this study, we dissected the roles of *KAT2A* in normal and malignant human hematopoiesis through analysis of the macromolecular complexes ATAC and SAGA, in which *KAT2A* exerts its HAT activity. We have aligned the roles of ATAC with maintenance of biosynthetic molecular activity, namely control of ribosomal protein and translation-associated genes. SAGA, on the other hand, participates in activation or maintenance of molecular programs underlying the characteristics of individual cell types, a property we equate with preservation of cell identity.

In the context of normal hematopoiesis, ATAC control of ribosomal protein genes selectively affects early stages of erythropoiesis, a lineage previously shown to be uniquely dependent on ribosomal assembly and rates of protein synthesis^{42,43} as captured by the selective erythroid defects of congenital ribosomopathies such as Diamond-Blackfan Anemia.⁴⁴ Selective loss of individual ribosomal proteins⁴⁵ or of global ribosomal protein regulators such as BMI1⁴⁶ have been shown to associate with proliferation and survival of early erythroid committed cells, with minimal changes to terminal differentiation. In the case of ATAC, the early nature of the defect may be potentiated by deregulation of the *EPOR* locus, a candidate instructor of erythroid lineage commitment.⁴⁷ However, the transcriptional consequences of reduced *EPOR* promoter acetylation upon ATAC loss are inconsistent, suggesting that it may contribute to rather than drive the erythroid defect. In the context of leukemia, ribosomal protein abundance and translational activity have been shown to sustain AML self-renewal.⁴² We found that ribosomal protein genes are selectively affected by loss of ATAC elements, which may nevertheless control other self-renewal

associated genes, namely the underlying *HOXA* signature associated with *KMT2A/MLL* rearrangements.

In contrast with the universal targeting of ribosomal protein genes by ATAC,^{21,37} SAGA may not regulate a constant set of genes but instead sustain the expression of the unique transcriptomes of individual cell types. This could in part be achieved through control of other transcriptional regulators as suggested by the functional ChIP enrichments in our data. In the context of normal hematopoiesis, SAGA may exert its putative identity control by fine-tuning normal progression of erythroid programs, a role for which its requirement may be contributory rather than absolute. The fact that SAGA, as indeed ATAC, requirements seem restricted to the erythroid lineage may reflect the distinctive nature of erythroid/megakaryocytic commitment and differentiation, which segregate from the stem cell root upstream of myeloid and lymphoid lineages^{48,49} with de novo establishment of transcription programs.⁵⁰ In the context of malignant hematopoiesis, SAGA participates in maintenance of the AML differentiation block, irrespective of the exact stage of cell differentiation, compatible with a general control of cell identity through preservation of existing transcriptional programs.⁵¹ Indeed, like *KAT2A* itself, we previously captured several SAGA elements (*SUPT20H*, *TRRAP*, *TAF5L*, *TAF6L*, and *TAF12*) as candidate genetic vulnerabilities in AML cell lines in a Clustered Regularly Interspaced Short Palindromic Repeats (CRISPR) drop-out screen.⁸ In contrast, we failed to capture ATAC components in the same screen,⁸ which nevertheless identified ribosomal proteins as universal vulnerabilities. One possible explanation is that cultured AML cell lines may be permissive to mild or moderate reduction in ribosomal assembly and protein synthesis. Our observed milder consequences to cell expansion of ATAC element loss are compatible with this view, as the screen readout⁸ was dependent on acute consequences to proliferation or survival. Also, the specific ATAC-mediated defect of *in vitro* self-renewal of CFCs is progressively displayed, becoming apparent upon colony replating but not affecting initial colony formation. Nevertheless, ATAC biosynthetic regulatory activities are required for supporting proliferation and, at least in some contexts self-renewal, of cells dependent on SAGA-mediated regulation through putative stabilization of their unique transcriptional programs. The resulting *KAT2A* activity can be described as preservation of the cellular status quo with minimal deviation toward alternative fate choices.

Preservation of the cellular status quo as the suggested operating mode of *KAT2A*-containing complexes is compatible with the role of *KAT2A* in sustaining rather than initiating gene transcription,⁵² as well as in stabilizing promoter activity and minimizing variability in transcriptional output as recently described by us in leukemia⁷ and ES cells.² Control of transcriptional variability by *KAT2A*-like acetyltransferases is well established in yeast GCN5,⁵³ which integrates a SAGA-like complex that was shown to regulate the global transcriptome.⁵⁴ Our⁷ and other⁵ observations in mammalian cells is that *Kat2a* only acetylates a subset of promoters, which are circumscribed into limited numbers of SAGA-specific and ATAC-specific targets (this paper and Krebs et al¹³). Although precise identification of *KAT2A* complex targets may be limited by the tools available, the number of promoters dependent on *KAT2A* for H3K9ac is restricted⁷ and functionally aligns with the categories we captured for ATAC and SAGA binding, suggesting a more restricted use in mammalian species as compared with yeast. Furthermore, our data suggest that ATAC and SAGA control of gene transcription may be more specific than control of promoter H3K9 acetylation, indicating

that specificity of transcriptional regulation by either complex may rely on unique effects of their additional enzymatic activities, namely H2B deubiquitination by USP22 and H4 acetylation by KAT14.⁵⁵ Accordingly, our inspection of USP22 requirements in erythropoiesis suggest that they align with the stage specificity of SAGA but may exceed the effects of loss of *SUPT20H* and more directly resemble postcommitment contributions of *KAT2A*. Future studies investigating single and combined requirements of ATAC and SAGA enzymatic subunits in locus and cellular regulation will enhance our understanding of the transcriptional control of cell state and fate decisions, including in leukemia and the normal blood system.

In respect of control of transcriptional variability, it is somewhat surprising that *Kat2a*-dependent promoters that respond to *Kat2a* KO with loss of H3K9ac and increased transcriptional variability are enriched in ATAC-dependent translation-associated genes⁷ and indeed enriched for ZZZ3 bound targets (ENCODE ChIP-seq significance tool; $P = 1.94e^{-4}$). Although both complexes regulate H3K9ac, control of transcriptional variability is conserved from yeast, which only contains a SAGA-like complex. One possibility is that ATAC and SAGA have evolved to nucleate distinct molecular functions of *KAT2A*. A more trivial explanation is that SAGA being preferentially recruited to cell type-specific promoters, comparison with ChIP-seq targets in different cell types may fail to detect enrichment despite a similar molecular regulation. Future analysis of transcriptional variability in response to parallel ATAC and SAGA-specific depletions in the same cell type should clarify this discrepancy. Additional studies will also be needed to understand the discrepancies between the identified requirements for *KAT2A* in human hematopoiesis and the broadly unperturbed hematopoietic development in the mouse. As we pointed out, detailed analysis of our own conditional *Kat2a* knockout model⁷ suggests a retention of MEP carrying unexcised *Kat2a* alleles, compatible with a requirement in erythroid specification. Also, we reported reduced mixed colony formation from HSC in *Kat2a* KO cells, which could portray a defect in early erythroid specification. We did not observe defective colony formation from MEP but cannot exclude these may have been masked by persistence of unexcised cells. On the other hand, a distinct conditional knockout model⁶ also failed to identify gross defects in hematopoiesis, although detailed analysis of lineage specification was not performed. To date, no other knockouts of ATAC and SAGA subunits have been investigated in the hematopoietic system, at the exception of *Usp22*, which did not affect stem and progenitor compartments or normal myeloid differentiation²⁷ but had a surprising tumor suppressor effect in *Kras*-driven transformation. However, a recent screen of deubiquitinating enzymes required for 4-week bone marrow engraftment that identified *Usp15* as a regulator of HSC activity *in vitro* and *in vivo*⁵⁶ also identified *Usp22*²⁷ as a possible hit, reinforcing the notion that additional analysis of ATAC and SAGA-mediated roles in mouse hematopoiesis is necessary.

In conclusion, we have identified unique requirements for ATAC and SAGA complexes in normal and leukemic hematopoiesis that are suggestive of respective pervasive roles in maintenance of biosynthetic activity and cell type-specific programs through complex-coordinated control of histone modifications and transcriptional stability. Individual cell types may be differentially dependent on the activity of either complex as suggested by a relatively stronger dependence on ATAC at early stages of erythropoiesis. Indeed, this may pose an opportunity for targeting of *KAT2A* activity through the

SAGA complex in leukemia. In support of the ATAC/SAGA functional dichotomy, a paper contemporary with this report identifies distinct targets and roles of ATAC and SAGA elements in mouse ES cells.⁵⁷ Similar to our findings, it associates ATAC with regulation of ribosomal protein genes and a pervasive control of pluripotency; SAGA, on the other hand, specifically regulates naïve pluripotency genes, akin to a role in cell identity. However, the authors find that SAGA and ATAC functional roles in mouse ES cells are independent of HAT activity,⁵⁷ which is distinct from our observations in the human hematopoietic system and, clearly, in AML. Detailed understanding of distinct chromatin regulatory strategies of SAGA and ATAC complexes for gene transcription and their usage in different cells will clarify the discrepancy. This knowledge can be explored for stability or perturbation of cell fate in regeneration and disease.

Acknowledgments

The authors thank the Cell Phenotyping Hub NIHR BRC, the University of Cambridge Department of Pathology Flow Sorting Facility, and Yanping Guo at the UCL Cancer Institute Flow Cytometry Translational Technology Platform for their expert support in cell sorting.

This work was funded by a Rosetrees Trust Studentship to L.A. (M650) and a Kay Kendall Leukaemia Fund Intermediate Fellowship (KKL888) to C.P. Work in the C.P. laboratory was also funded by a Leukaemia John Goldman Fellowship for Future Science (2017) and a Wellcome Trust/University of Cambridge ISSF Grant to C.P. S.G. was funded by a Lady Tata Memorial Trust Studentship, a Trinity Henry Barlow Trust Studentship, and by the Cambridge Trust. This study was also supported by an NIH RO1 grant (1R01GM131626-01) to L.T., by Agence Nationale de la Recherche (ANR) Program grants, AAPG2019 PICen to L.T., ANR PRCI AAPG2019 EpiCAST to L.T., grant ANR-10-LABX-0030-INRT, and a French State fund managed by the ANR under the frame program Investissements d'Avenir ANR-10IDEX-0002-02 to Institut de Genetique et de Biologie Moleculaire et Cellulaire (IGBMC). Samples were provided by the Cambridge Blood and Stem Cell Biobank, which is supported by the Cambridge NIHR BRC Wellcome Trust MRC Stem Cell Institute and the Cambridge Experimental Cancer Medicine Centre, UK.

Authorship

Contribution: C.P. conceived the study; L.A. and C.P. designed the study; L.A., E.F., S.W., A.F.D., G.G., S.K., M.M.-S., H.D., A. Chandru, R.A., R.S., and S.G. collected and assembled data; G.G., D.F., A. Curti, E.S., B.J.P.H., and L.T. contributed critical reagents; L.A., E.F., S.W., R.K., and C.P. analyzed data; L.A. and C.P. interpreted data; L.A. and C.P. wrote the manuscript; and all authors approved the final version of the manuscript.

Conflict-of-interest disclosure: The authors declare no competing financial interests.

ORCID profiles: S.W., 0000-0002-1064-4198; G.G., 0000-0003-1390-6592; R.A., 0000-0001-5077-3798; B.J.P.H., 0000-0003-0312-161X; L.T., 0000-0001-7398-2250.

Correspondence: Cristina Pina, College of Health, Medicine and Life Sciences, Division of Biosciences, Brunel University London, Uxbridge UB8 3PH, United Kingdom; e-mail: cristina.pina@brunel.ac.uk.

References

1. Xu W, Edmondson DG, Evrard YA, Wakamiya M, Behringer RR, Roth SY. Loss of Gcn5l2 leads to increased apoptosis and mesodermal defects during mouse development. *Nat Genet.* 2000;26(2):229-232.
2. Moris N, Edri S, Seyres D, et al. Histone acetyltransferase KAT2A stabilizes pluripotency with control of transcriptional heterogeneity. *Stem Cells.* 2018;36(12):1828-1838.
3. Martínez-Cerdeño V, Lemen JM, Chan V, et al. N-Myc and GCN5 regulate significantly overlapping transcriptional programs in neural stem cells. *PLoS One.* 2012;7(6):e39456.
4. Gao B, Kong Q, Zhang Y, et al. The histone acetyltransferase Gcn5 positively regulates T cell activation. *J Immunol.* 2017;198(10):3927-3938.
5. Wang Y, Yun C, Gao B, et al. The lysine acetyltransferase GCN5 is required for iNKT cell development through EGR2 acetylation. *Cell Rep.* 2017;20(3):600-612.
6. Bararia D, Kwok HS, Welner RS, et al. Acetylation of C/EBP α inhibits its granulopoietic function. *Nat Commun.* 2016;7(1):10968.
7. Domingues AF, Kulkarni R, Giotopoulos G, et al. Loss of Kat2a enhances transcriptional noise and depletes acute myeloid leukemia stem-like cells. *eLife.* 2020;9:e51754.
8. Tzelepis K, Koike-Yusa H, De Braekeleer E, et al. A CRISPR dropout screen identifies genetic vulnerabilities and therapeutic targets in acute myeloid leukemia. *Cell Rep.* 2016;17(4):1193-1205.
9. Brownell JE, Zhou J, Ranalli T, et al. Tetrahymena histone acetyltransferase A: a homolog to yeast Gcn5p linking histone acetylation to gene activation. *Cell.* 1996;84(6):843-851.
10. Grant PA, Duggan L, Côté J, et al. Yeast Gcn5 functions in two multisubunit complexes to acetylate nucleosomal histones: characterization of an Ada complex and the SAGA (Spt/Ada) complex. *Genes Dev.* 1997;11(13):1640-1650.
11. Wang Y, Guo YR, Liu K, et al. KAT2A coupled with the α -KGDH complex acts as a histone H3 succinyltransferase. *Nature.* 2017;552(7684):273-277.
12. Spedale G, Timmers HTM, Pijnappel WWMP. ATAC-king the complexity of SAGA during evolution. *Genes Dev.* 2012;26(6):527-541.
13. Krebs AR, Karmodiya K, Lindahl-Allen M, Struhl K, Tora L. SAGA and ATAC histone acetyl transferase complexes regulate distinct sets of genes and ATAC defines a class of p300-independent enhancers. *Mol Cell.* 2011;44(3):410-423.
14. Riss A, Scheer E, Joint M, Trowitzsch S, Berger I, Tora L. Subunits of ADA-two-A containing (ATAC) or Spt-Ada-Gcn5-acetyltransferase (SAGA) coactivator complexes enhance the acetyltransferase activity of GCN5. *J Biol Chem.* 2015;290(48):28997-29009.
15. Liu G, Zheng X, Guan H, et al. Architecture of *Saccharomyces cerevisiae* SAGA complex. *Cell Discov.* 2019;5(1):25.
16. Wang H, Dienemann C, Stützer A, Urlaub H, Cheung ACM, Cramer P. Structure of the transcription coactivator SAGA. *Nature.* 2020;577(7792):717-720.
17. Papai G, Frechard A, Kolesnikova O, Crucifix C, Schultz P, Ben-Shem A. Structure of SAGA and mechanism of TBP deposition on gene promoters. *Nature.* 2020;577(7792):711-716.
18. Carré C, Ciurciu A, Komonyi O, et al. The Drosophila NURF remodelling and the ATAC histone acetylase complexes functionally interact and are required for global chromosome organization. *EMBO Rep.* 2008;9(2):187-192.
19. Sugauma T, Gutiérrez JL, Li B, et al. ATAC is a double histone acetyltransferase complex that stimulates nucleosome sliding. *Nat Struct Mol Biol.* 2008;15(4):364-372.
20. Helmlinger D, Tora L. Sharing the SAGA. *Trends Biochem Sci.* 2017;42(11):850-861.
21. Mi W, Guan H, Lyu J, et al. YEATS2 links histone acetylation to tumorigenesis of non-small cell lung cancer. *Nat Commun.* 2017;8(1):1088.
22. Guelman S, Kozuka K, Mao Y, et al. The double-histone-acetyltransferase complex ATAC is essential for mammalian development. *Mol Cell Biol.* 2009;29(5):1176-1188.
23. Koutelou E, Hirsch CL, Dent SY. Multiple faces of the SAGA complex. *Curr Opin Cell Biol.* 2010;22(3):374-382.
24. McMahon SB, Van Buskirk HA, Dugan KA, Copeland TD, Cole MD. The novel ATM-related protein TRRAP is an essential cofactor for the c-Myc and E2F oncoproteins. *Cell.* 1998;94(3):363-374.
25. Schrecengost RS, Dean JL, Goodwin JF, et al. USP22 regulates oncogenic signaling pathways to drive lethal cancer progression. *Cancer Res.* 2014;74(1):272-286.
26. Kosinsky RL, Helms M, Zerche M, et al. USP22-dependent HSP90AB1 expression promotes resistance to HSP90 inhibition in mammary and colorectal cancer. *Cell Death Dis.* 2019;10(12):911.
27. Melo-Cardenas J, Xu Y, Wei J, et al. USP22 deficiency leads to myeloid leukemia upon oncogenic Kras activation through a PU.1-dependent mechanism. *Blood.* 2018;132(4):423-434.
28. Pina C, May G, Soneji S, Hong D, Enver T. MLLT3 regulates early human erythroid and megakaryocytic cell fate. *Cell Stem Cell.* 2008;2(3):264-273.
29. Sutherland JA, Turner AR, Mannoni P, McGann LE, Turc JM. Differentiation of K562 leukemia cells along erythroid, macrophage, and megakaryocyte lineages. *J Biol Response Mod.* 1986;5(3):250-262.

30. Lam LT, Ronchini C, Norton J, Capobianco AJ, Bresnick EH. Suppression of erythroid but not megakaryocytic differentiation of human K562 erythroleukemic cells by notch-1. *J Biol Chem.* 2000;275(26):19676-19684.
31. de Thonel A, Vandekerckhove J, Lanneau D, et al. HSP27 controls GATA-1 protein level during erythroid cell differentiation. *Blood.* 2010;116(1):85-96.
32. Kuvardina ON, Herglotz J, Kolodziej S, et al. RUNX1 represses the erythroid gene expression program during megakaryocytic differentiation. *Blood.* 2015;125(23):3570-3579.
33. Xie Y, Gao L, Xu C, et al. ARHGEF12 regulates erythropoiesis and is involved in erythroid regeneration after chemotherapy in acute lymphoblastic leukemia patients. *Haematologica.* 2020;105(4):925-936.
34. Kuleshov MV, Jones MR, Rouillard AD, et al. Enrichr: a comprehensive gene set enrichment analysis web server 2016 update. *Nucleic Acids Res.* 2016;44(W1):W90-W97.
35. Merryweather-Clarke AT, Atzberger A, Soneji S, et al. Global gene expression analysis of human erythroid progenitors. *Blood.* 2011;117(13):e96-e108.
36. Tusi BK, Wolock SL, Weinreb C, et al. Population snapshots predict early haematopoietic and erythroid hierarchies. *Nature.* 2018;555(7694):54-60.
37. Mi W, Zhang Y, Lyu J, et al. The ZZ-type zinc finger of ZZZ3 modulates the ATAC complex-mediated histone acetylation and gene activation. *Nat Commun.* 2018;9(1):3759.
38. Goardon N, Marchi E, Atzberger A, et al. Coexistence of LMPP-like and GMP-like leukemia stem cells in acute myeloid leukemia. *Cancer Cell.* 2011;19(1):138-152.
39. Gu TL, Goss VL, Reeves C, et al. Phosphotyrosine profiling identifies the KG-1 cell line as a model for the study of FGFR1 fusions in acute myeloid leukemia. *Blood.* 2006;108(13):4202-4204.
40. Larizza L, Magnani I, Beghini A. The Kasumi-1 cell line: a t(8;21)-kit mutant model for acute myeloid leukemia. *Leuk Lymphoma.* 2005;46(2):247-255.
41. Schuringa JJ, Schepers H. Ex vivo assays to study self-renewal and long-term expansion of genetically modified primary human acute myeloid leukemia stem cells. *Methods Mol Biol.* 2009;538:287-300.
42. Signer RA, Magee JA, Salic A, Morrison SJ. Haematopoietic stem cells require a highly regulated protein synthesis rate. *Nature.* 2014;509(7498):49-54.
43. Magee JA, Signer RAJ. Developmental stage-specific changes in protein synthesis differentially sensitize hematopoietic stem cells and erythroid progenitors to impaired ribosome biogenesis. *Stem Cell Reports.* 2021;16(1):20-28.
44. Khajuria RK, Munschauer M, Ulirsch JC, et al. Ribosome levels selectively regulate translation and lineage commitment in human hematopoiesis. *Cell.* 2018;173(1):90-103.e19.
45. Miyake K, Utsugisawa T, Flygare J, et al. Ribosomal protein S19 deficiency leads to reduced proliferation and increased apoptosis but does not affect terminal erythroid differentiation in a cell line model of Diamond-Blackfan anemia. *Stem Cells.* 2008;26(2):323-329.
46. Gao R, Chen S, Kobayashi M, et al. Bmi1 promotes erythroid development through regulating ribosome biogenesis. *Stem Cells.* 2015;33(3):925-938.
47. Grover A, Mancini E, Moore S, et al. Erythropoietin guides multipotent hematopoietic progenitor cells toward an erythroid fate. *J Exp Med.* 2014;211(2):181-188.
48. Carrelha J, Meng Y, Kettle LM, et al. Hierarchically related lineage-restricted fates of multipotent haematopoietic stem cells. *Nature.* 2018;554(7690):106-111.
49. Belluschi S, Calderbank EF, Ciaurro V, et al. Myelo-lymphoid lineage restriction occurs in the human haematopoietic stem cell compartment before lymphoid-primed multipotent progenitors. *Nat Commun.* 2018;9(1):4100.
50. Notta F, Zandi S, Takayama N, et al. Distinct routes of lineage development reshape the human blood hierarchy across ontogeny. *Science.* 2016;351(6269):aab2116.
51. Arede L, Pina C. Buffering noise: KAT2A modular contributions to stabilization of transcription and cell identity in cancer and development. *Exp Hematol.* 2021;93:25-37.
52. Jin Q, Yu LR, Wang L, et al. Distinct roles of GCN5/PCAF-mediated H3K9ac and CBP/p300-mediated H3K18/27ac in nuclear receptor transactivation. *EMBO J.* 2011;30(2):249-262.
53. Raser JM, O'Shea EK. Control of stochasticity in eukaryotic gene expression. *Science.* 2004;304(5678):1811-1814.
54. Baptista T, Grünberg S, Minoungou N, et al. SAGA is a general cofactor for RNA polymerase II transcription [published correction appears in *Mol Cell.* 2018;70(6):1163-1164]. *Mol Cell.* 2017;68(1):130-143.e5.
55. Orpinell M, Fournier M, Riss A, et al. The ATAC acetyl transferase complex controls mitotic progression by targeting non-histone substrates. *EMBO J.* 2010;29(14):2381-2394.
56. van den Berk P, Lancini C, Company C, et al. USP15 deubiquitinase safeguards hematopoiesis and genome integrity in hematopoietic stem cells and leukemia cells. *Cell Rep.* 2020;33(13):108533.
57. Fischer V, Plassard D, Ye T, et al. The related coactivator complexes SAGA and ATAC control embryonic stem cell self-renewal through acetyltransferase-independent mechanisms. *Cell Rep.* 2021;36(8):109598.